

## Measuring Velocity and Acceleration Using Doppler Shift of a Source with an Example of Jet in SS433

Sanjay M. Wagh

*Central India Research Institute, 34, Farmland, Ramdaspath, Nagpur 440 010, India.*

*e-mail: waghsm.ngp@gmail.com*

Received 13 October 2013; accepted 13 June 2014

**Abstract.** We describe here as to how the Doppler shift of a source needs to be used to measure its velocity and acceleration. We also apply this method, as an example here, to spectral lines of the blue-shifted jet in micro-quasar SS433 and discuss the intricacies of these measurements.

*Key words.* Doppler effect—measuring velocity and acceleration of the source—jet in SS433.

### 1. Introduction

Recently, we showed that the Doppler shift of a source must necessarily include contribution from its acceleration, apart from that due to its velocity (Wagh 2013a). We also discussed certain implications of this result (Wagh 2013b, c). Here, we discuss the measurements of velocity and acceleration of the source from its Doppler shift.

For completeness, we first recall the derivation of the Doppler shift from Wagh (2013a). We emphasize that this analysis of Doppler's effect holds in all the possible situations of the relative motion of the source of light and the observer.

Doppler's discovery is that if a source of a (monochromatic) wave is in motion relative to an observer, then the observed wavelength of this wave must be different than that emitted by the source. The Doppler shift results from only the relative motion of the source and the observer. From the Doppler shift of a source, we can infer the nature of its motion with respect to us.

Figure 1(a) shows a stationary source  $S$  emitting a monochromatic wave whose crest meets an observer at point  $O$  at time  $t = 0$ , at which instant the subsequent crest is then lagging at point  $M$ , located at a distance  $cT$  behind the point  $O$  along the line  $SO$ . Here,  $T$  is the period of the wave and  $c$  is the speed of the wave (for light, in vacuum).

Let the observer at  $O$  move with velocity  $\vec{v}$  making an angle  $\theta$  with the line  $SO$  and acceleration  $\vec{a}$  at  $t = 0$ , as shown in Figure 1(a). (In general, velocity and acceleration can be differently directed.) Furthermore, let the wave at  $M$  reach the observer at point  $P$  after lapse  $T'$  of time.

Actually, a ray from  $S$  passing through the point  $Q$  on the wavefront at  $M$  reaches the observer at time  $T'$ , as is shown in Figure 1(a). But, the angle  $\phi = \angle MSQ$



acceleration, as adopted in the following, are incidental to obtaining manageable equations.

Now, for time interval equal to the period of the wave, constancy of the acceleration may be a good approximation in situations of our interest.

For constant acceleration  $\vec{a}$  and initial velocity  $\vec{u}$ , the geometry now dictates that

$$(cT')^2 = \left(uT' + \frac{1}{2}aT'^2\right)^2 \sin^2 \theta + \left[cT + \left(uT' + \frac{1}{2}aT'^2\right) \cos \theta\right]^2. \quad (3)$$

On manipulating this equation, in terms of the observed frequency  $\nu_o = 1/T'$  and the emitted frequency  $\nu_e = 1/T$ , we have

$$\nu_o^4 + (2\beta\nu_e \cos \theta)\nu_o^3 - \left[(1 - \beta^2)\nu_e^2 - \alpha\nu_e \cos \theta\right]\nu_o^2 + \alpha\beta\nu_e^2\nu_o + \frac{\alpha^2}{4}\nu_e^2 = 0, \quad (4)$$

where we have set  $\alpha = a/c$  and  $\beta = u/c$ .

To first order in  $\alpha$  and neglecting the term with product  $\alpha\beta$ , the observed frequency is obtained using equation (4) as

$$\begin{aligned} \nu_o &= \nu_e \left[ \sqrt{1 - \beta^2 \sin^2 \theta - \left(\frac{\alpha}{\nu_e}\right) \cos \theta - \beta \cos \theta} \right] \\ &\approx \nu_e \left[ 1 - \frac{\beta^2}{2} \sin^2 \theta - \beta \cos \theta \right] - \frac{\alpha}{2} \cos \theta. \end{aligned} \quad (5)$$

In section 2, we will focus on formula (5) for further analysis. Also, refer to the analysis in [Appendix](#) corresponding to the case of uniform velocity, and note that the standard Doppler shift expression (A1) disagrees with equation (5) when  $\alpha = 0$ .

## 2. Strategy underlying measurement: Constant acceleration

Consider that the source under considerations is emitting two spectral lines at frequencies  $\nu_{e(1)}$  and  $\nu_{e(2)}$  and the corresponding observed frequencies are  $\nu_{o(1)}$  and  $\nu_{o(2)}$ , respectively. Then, using equation (5), we obtain

$$\begin{aligned} f(\beta, \theta) \equiv 1 - \frac{\beta^2}{2} \sin^2 \theta - \beta \cos \theta &= \frac{\nu_{o(2)} - \nu_{o(1)}}{\nu_{e(2)} - \nu_{e(1)}} \\ &= \left[ \frac{\lambda_{o(1)} - \lambda_{o(2)}}{\lambda_{e(1)} - \lambda_{e(2)}} \right] \times \frac{\lambda_{e(1)}\lambda_{e(2)}}{\lambda_{o(1)}\lambda_{o(2)}}, \end{aligned} \quad (6)$$

where the  $\lambda$ 's are the corresponding wavelengths.

The function  $f(\beta, \theta) = 1 - (\beta^2 \sin^2 \theta/2) - \beta \cos \theta$  is then the quantity measured here in terms of the observed and emitted frequencies or wavelengths, and this function is plotted in Fig. 2 as a surface.

At this point, notice that for angular ranges  $\sim[0, 110^\circ]$  and  $\sim[240^\circ, 360^\circ]$ , we have  $f(\beta, \theta) < 1$ ; and within the angular range  $\sim[110^\circ, 240^\circ]$ , we have  $2 \geq f(\beta, \theta) > 1$ . We stress that  $f > 1$  does not necessarily mean relativistic velocity. These ranges also overlap: for  $[90^\circ, 110^\circ]$  and  $[250^\circ, 270^\circ]$ ,  $f > 1$  and  $f < 1$ .

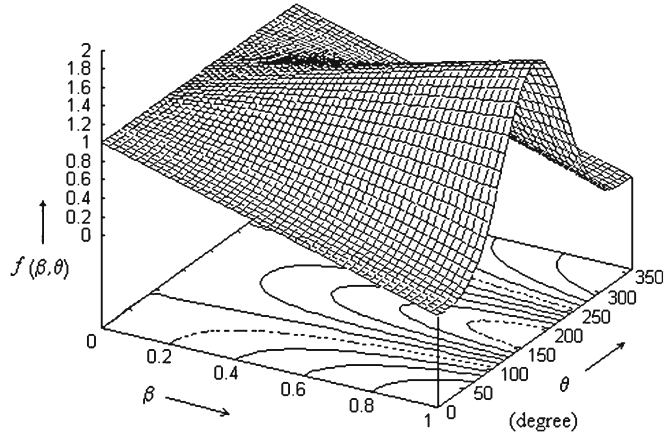


**Figure 2.** Function  $f(\beta, \theta)$  in equation (6) as a surface.

Notice also that when  $f(\beta, \theta) \neq 1$ , there exists a ‘non-zero’ lower bound,  $\beta_{\min}$ , for velocity  $\beta$ . For  $f < 1$ ,  $\beta_{\min} = 1 - f$  and for  $f > 1$ ,  $\beta_{\min} = f - 1$ . For convenience, we then plot the contours of  $f(\beta, \theta) = \text{constant}$  in Fig. 3. For  $f(\beta, \theta) = 1$ ,  $\beta_{\min} = 0$  because  $\beta = 0$  for all values of the angle  $\theta$ . Importantly, for  $f(\beta, \theta) \approx 1$ , velocity can be non-relativistic over a large angular range. Then, from the observational data of  $(\lambda_{e(1)}, \lambda_{e(2)}, \lambda_{o(1)}, \lambda_{o(2)})$ , we obtain the ‘observed’ value of  $f(\beta, \theta)$ , which we denote by  $\{f\}$ .

Now, from equation (5), we have

$$\frac{\alpha}{2c} \cos \theta = \frac{\{f\}}{\lambda_e} - \frac{1}{\lambda_o} \tag{7}$$

and, as we are using the ‘observed’ quantities, this is then the ‘observed’ value. We denote this observed value by  $\{\alpha \cos \theta / 2c\}$ .

From the data related to just a pair of spectral lines, we can then infer the values of  $f$ ,  $\beta_{\min}$  and  $(\alpha \cos \theta) / 2c$ . Furthermore, from  $f > 1$  or  $f < 1$ , we can also infer as to how the material emitting that pair of lines is, likely to be, angularly situated.

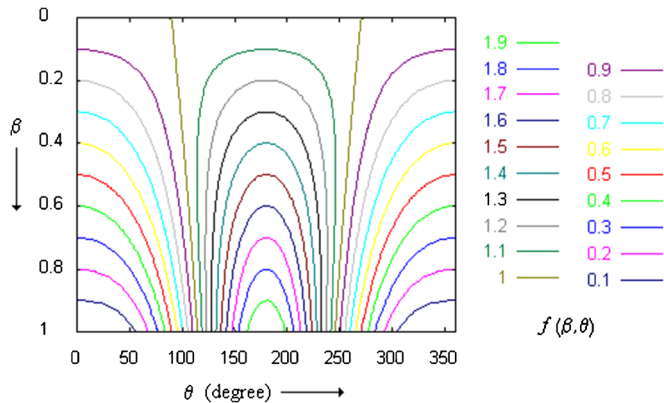


**Figure 3.**  $\beta$  as a function of  $\theta$  for various values of  $f(\beta, \theta)$ .

Of course, this information can be considered to be ‘reliable’ only if that pair of spectral lines is emitted by the ‘same’ material, with the reality of this situation not being decidable on the basis of that information.

For more than a pair of spectral lines, we note that error in the observed value of  $f(\beta, \theta)$  obtained for a selected pair of lines ‘naturally’ provides us the basis for further analysis in the following manner.

To fix ideas, let

$$f = f_0 \pm \delta f \quad (8)$$

for a ‘specific’ pair of spectral lines ( $\lambda_{e(1)}, \lambda_{e(2)}$ ).

Now, all other spectral lines whose function  $f$ , evaluated using the line of wavelength  $\lambda_{e(1)}$ , has values in the range  $[f_0 + \delta f, f_0 - \delta f]$  can be considered to be emitted by the material moving ‘similarly’ to that emitting the first spectral line  $\lambda_{e(1)}$ . These lines possess ‘differing’ values of  $\beta_{\min}$ , in general. Each  $\beta_{\min}$  will have associated error of  $\pm \delta f$ . For consistency with the existence of the minimum value of velocity  $\beta_{\min}$  for  $f(\beta, \theta) \neq 1$ , it is required that the material emitting these lines to be moving with speed corresponding to the ‘maximum’ value ( $\max \beta_{\min}$ ), of  $\beta_{\min}$ ; and will then have corresponding error.

Here, ( $\max \beta_{\min}$ ) is the ‘smallest’ value of the speed  $\beta$  with which the material can be moving and emitting the spectral lines under considerations. We may then use it as ‘the value’ of  $\beta$  (with corresponding error) in the expression for the function  $f(\beta, \theta)$  to infer the angle of motion of the material emitting the line as

$$\cos \theta = \frac{1}{(\max \beta_{\min})} \left( 1 - \sqrt{1 + (\max \beta_{\min})^2 + 2(f - 1)} \right). \quad (9)$$

The observed value of  $(\alpha/2c) \cos \theta$  as in eq. (7) then provides us the value of acceleration of the material emitting the line. Corresponding values of angle  $\theta$  then provide us the angular spread of the material emitting these lines.

Of course, the analysis is certainly much more complicated than that presented above. In reality, different pairs of lines from a source will yield drastically differing results for the above analysis. In particular, the angles obtained with one pair of lines will be seen to be quite different when another pair of lines is used. Nevertheless, the following part of the strategy emerges on relevant considerations.

Then, a pair of lines that accommodates maximum number of other lines from the source within its error limits for function  $f(\beta, \theta)$  will, most likely, be representing the source. This is so because lines from a multi-temperature plasma moving at bulk speed  $\beta$  and accelerating/decelerating at rate  $\alpha$  can be expected to show this feature. Note also that results for angles obtained with the acceleration term need to be in ‘general conformity’ with those obtained without it.

We now turn to the example of the blue-shifted jet in micro-quasar SS433.

### 3. Example of the blue-shifted jet in micro-quasar SS433

SS433 shows (Margon 1984; Mirabel 1999; Margon & Anderson 1989; Fabrika 2004) emission lines from ionized gas in a highly collimated jet ejected by a compact object and is a member of the ‘micro-quasar’ class of X-ray binaries. The ‘kinematic model’ of SS433 (Margon & Anderson 1989) describes Doppler shifts of the blue- and red-shifted  $H_\alpha$  lines as a result of a pair of oppositely directed precessing jets

with speed,  $v_J = 0.26c$ . As per this analysis, the jet in SS433 precesses with a 162.5 day period in a cone with half-angle of  $19.85^\circ$  about an axis which is  $78.83^\circ$  to the line-of-sight. Marshall *et al.* (2013) also reported multi-wavelength observations of the Jet in SS433.

In what follows, we show how the acceleration dependence of the Doppler shift changes the estimate of the speed of the jet.

From Table 4 in Marshall *et al.* (2013), consider the line Fe XXV of rest wavelength  $\lambda_{e(1)} = 1.855 \text{ \AA}$  and observed wavelength  $\lambda_{o(1)} = 1.86 \pm 0.001 \text{ \AA}$ , and line Fe XXVI of rest wavelength  $\lambda_{e(2)} = 1.78 \text{ \AA}$  and observed wavelength  $\lambda_{o(2)} = 1.786 \pm 0.001 \text{ \AA}$ .

Then, for the pair of these lines, we have

$$\{f\} = 0.981 \pm 0.001, \quad \beta_{\min} = 0.019 \pm 0.001, \quad \beta_{\perp} = 0.195 \pm 0.005$$

$$\beta_{78.83^\circ} = 0.082 \pm 0.004, \quad \left\{ \frac{\alpha}{2} \cos \theta \right\} = -0.0088 \pm 0.0001.$$

We may then conclude that the material emitting the Fe XXV and Fe XXIV lines in the blue-shifted jet of SS433 is moving with speed  $\sim 0.08c$  and is decelerating.

Considering the next two emission lines S XVI ( $\lambda_{e(1)} = 4.729 \text{ \AA}$ ,  $\lambda_{o(1)} = 4.735 \pm 0.001 \text{ \AA}$ ) and S XV ( $\lambda_{e(2)} = 5.055 \text{ \AA}$ ,  $\lambda_{o(2)} = 5.050 \pm 0.002 \text{ \AA}$ ) of sulphur S, we have

$$\{f\} = 0.966 \pm 0.003, \quad \beta_{\min} = 0.034 \mp 0.003, \quad \beta_{\perp} = 0.261 \pm 0.044$$

$$\beta_{78.83^\circ} = 0.132 \pm 0.001, \quad \left\{ \frac{\alpha}{2} \cos \theta \right\} = -0.007 \pm 0.001.$$

We may then conclude that the material emitting the S XVI and S XV lines in the blue-shifted jet of SS433 is moving with speed  $\sim 0.13c$  and is decelerating. However, for the same angle, it is moving somewhat faster and decelerating somewhat slower than the material of the jet emitting the Fe XXV and Fe XXIV lines.

But, aforementioned conclusions are entirely premature, for they have been obtained using only a pair of spectral lines. There is no way we can be sure about the commonness of the material emitting the pair under considerations!

A proper analysis then uses (Wagh & Sarwe 2013) the bounds on function  $f(\beta, \theta)$  from a pair of lines to determine which lines have their  $f$ -value within these bounds, checks for the consistency of the results with the angular distribution obtained without the acceleration-dependence of the Doppler shifts, etc.

In this analysis, it is however seen (Wagh & Sarwe 2013) that the value of acceleration obtained for the material of the jet in SS433 is unreasonably large. This is an indication that the constancy of acceleration as is used to obtain eq. (5) is not a good approximation in the situation under consideration. Consequently, it is then necessary to consider variable acceleration. The next section therefore describes the relevant strategy.

#### 4. Strategy with temporally variable acceleration

Let us consider the simple situation of acceleration varying sinusoidally with time. This is not any unreasonable assumption, for a train carriage being pulled or pushed by an engine exhibits this feature. As the coupling between the engine and the

carriage slackens, friction at the rails decelerates the carriage; and when it gets taut, carriage accelerates due to the pull/push of the engine. This process repeats periodically, as the engine pulls/pushes the train. We expect it also in systems like SS433, wherein the mechanisms of acceleration and deceleration of the material are operating simultaneously. The material of the jet is being pushed from behind by the material ejected by the prime mover at a later time and is being obstructed by material the jet is ramming into.

Then, let the temporal rate of acceleration be given by

$$\frac{da}{dt} = a_0 \sin(\omega t), \quad a_0 = \text{constant.} \quad (10)$$

Then, on integration, we obtain

$$(\text{SP}) = \frac{a_0}{\omega^3} \cos(\omega t) + k_1 \frac{t^2}{2} + k_2 t + k_3, \quad (11)$$

where  $k_1, k_2, k_3$  are integration constants. When the frequency  $\omega$  is appropriately small, we may approximate the cosine term and obtain

$$(\text{SP}) = \frac{a_0}{\omega^3} + \left(k_1 - \frac{a_0}{\omega}\right) \frac{t^2}{2} + k_2 t + k_3. \quad (12)$$

Substituting this in eq. (2), we then obtain after suitable manipulations:

$$v_o \approx f(\beta, \theta) v_e - \frac{1}{c} \left(k_3 + \frac{a_0}{\omega^3}\right) v_e^2 \cos \theta - \frac{1}{2c} \left(k_1 - \frac{a_0}{\omega}\right) \cos \theta, \quad (13)$$

where  $f(\beta, \theta)$  is as defined earlier with  $k_2 = \beta c$ , and have retained only the first order terms in acceleration. We set  $k_1 = 0$  and  $k_3 = 0$ . (Notice that we recover the analysis with constant acceleration when  $k_1 \neq 0$  and in the (obvious) situation of  $a_0 = 0$ .)

Now, let  $\Delta v_o = v_{o(1)} - v_{o(2)}$ ,  $\Delta v_e = v_{e(1)} - v_{e(2)}$ ,  $\Delta(v_e^2) = (v_{e(1)})^2 - (v_{e(2)})^2$ . Then, from eq. (13), we have

$$\left(\frac{\Delta v_o}{\Delta v_e}\right) = f(\beta, \theta) + h(a_0, \omega, \theta) \left(\frac{\Delta(v_e^2)}{\Delta v_e}\right), \quad (14)$$

where we have set  $h(a_0, \omega, \theta) = -(a_0/\omega^3 c) \cos \theta$ . This equation is ‘linear’ in  $(\Delta v_o/\Delta v_e)$  and  $(\Delta(v_e^2)/\Delta v_e) \equiv v_{e(1)} + v_{e(2)}$ . From the observational data  $(v_e, v_o)$  or, equivalently,  $(\lambda_e, \lambda_o)$ , we can then obtain  $f(\beta, \theta)$  and  $h(a_0, \omega, \theta)$  by linear regression. The acceleration  $a_0/\omega$  of the emitter can then be estimated.

Velocity  $\beta_{\min}$ , corresponding to the above  $f(\beta, \theta)$ , provides us the minimum velocity with which the material emitting frequency  $v_{e(1)}$  of the jet is moving. For the mean jet speed, we may select the average of  $\beta_{\min}$  or  $(\max \beta_{\min})$ , and this value is ‘added’ to each  $\beta_{\min}$ . Then, angle  $\theta$  can be obtained from the  $f$ -values as before. We thus obtain the ‘observational parameters’ of the kinematics of the material of the jet. Of course, details depend on the parameter  $\omega$  and further work is necessary to arrive at a satisfactory model.

Nevertheless, we note the following: The order of the term  $(\Delta v_o/\Delta v_e)$  is unity and so is that of  $f(\beta, \theta)$ . Then, as the order of the quantity  $(\Delta(v_e^2)/\Delta v_e)$  is  $10^8 c$ ,

the order of the quantity  $h(a_0, \omega, \theta)$  is  $10^{-8}c^{-1}$ . Thus, the acceleration  $a_0/\omega$  is of order  $10^{-8}\omega^2$ , which is a reasonable value. Then, the last term of eq. (13) will be negligible. We may note that the time-scale of change in velocity is now of the order of  $\beta c/(a_0/\omega) \sim \beta c 10^8/\omega^2$ .

## 5. Concluding remarks

In summary, Doppler shifts of spectral lines lead to measurements of the velocity and acceleration of the material emitting them. Noticeably, our method of deriving the Doppler shift accommodates situations of constant velocity, constant acceleration and that of variable acceleration by way of eq. (2), as shown. We have also discussed an astrophysical example of the blue-shifted jet from a micro-quasar SS433, including the intricacies of these measurements when the acceleration is variable. The method is, of course, more general than just this application to the jet in SS433.

Since our purpose was to discuss method(s) of measuring velocity and acceleration of a source using the Doppler shift, we do not provide here the details of jet in SS433, which will be found in Wagh and Sarwe (2013).

## Acknowledgements

The author would like to thank the anonymous referee for raising the issues of the [Appendix](#) and for other useful as well as helpful suggestions.

## Appendix

The ‘usual’ Doppler shift formula is (see, for example, French 1966):

$$v_o = v_e \frac{\sqrt{1 - \beta^2}}{1 + \beta \cos \theta}. \quad (\text{A1})$$

This formula has also received experimental validation, for example, in many cosmic ray experiments involving relativistically moving charged particles emitting radiation. We recall the derivation of this formula that is based on the following diagram:

Figure A1(a) shows a stationary source emitting ‘first’ pulse at time  $t_1$  and the ‘second’ pulse at time  $t_2$ , the time measured in the frame of the source. The frequency of emission is then  $1/(t_2 - t_1)$ . The ‘initial’ line-of-sight (SO), is shown making an angle  $\bar{\theta}$  with the Y-axis. When the first pulse reaches the observer at O, time elapsed is  $T_1 = t_1 + (\text{SO})/c$ .

Let the observer move along the line OP making an angle  $\bar{\phi}$  with the X-axis, with P being the point at which the second pulse reaches the observer at time  $T_2 = t_2 + (\text{SP})/c$ . Then,

$$T_2 - T_1 = t_2 + (\text{SP})/c - t_1 - (\text{SO})/c \quad (\text{A2})$$

With  $(\text{SO}) = \sqrt{x_1^2 + y_1^2}$ ,  $(\text{SP})^2 = \sqrt{(x_1 + \delta x)^2 + (y_1 + \delta y)^2}$ ,  $x_1 \gg \delta x$ ,  $y_1 \gg \delta y$ , we get

$$T_2 - T_1 \approx t_2 - t_1 + \cos \bar{\theta} \delta x + \sin \bar{\theta} \delta y \quad (\text{A3})$$

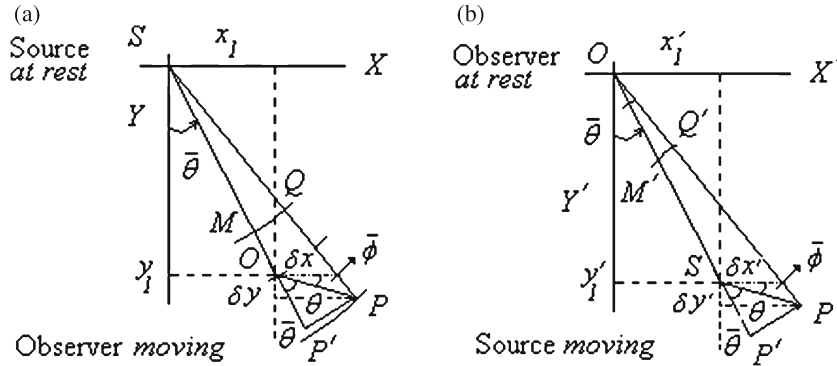


Figure A1(a, b). Geometry for 'usual' formula of Doppler shift.

But,  $\delta x = (OP) \cos \bar{\phi}$  and  $\delta y = (OP) \sin \bar{\phi}$ ; and we get to first order

$$T_2 - T_1 \approx t_2 - t_1 + \frac{(OP)}{c} \cos(\bar{\theta} + \bar{\phi}) \equiv t_2 - t_1 + \frac{(OP)}{c} \cos \theta$$

$$c\Delta T = c\Delta t + (OP) \cos \theta, \quad (\text{A4})$$

where  $\theta$  is the angle line  $OP$  makes with line  $SO$ .

If we consider the observer to be stationary and source to be moving, considerations similar to those of the above applied to of Fig. A1(b) then yield to first order:

$$T'_2 - T'_1 \approx t'_2 - t'_1 + \frac{(SP)}{c} \cos(\bar{\theta} + \bar{\phi}) \equiv t'_2 - t'_1 + \frac{(SP)}{c} \cos \theta$$

$$c\Delta T' = c\Delta t' + (SP) \cos \theta. \quad (\text{A5})$$

We distinguish the time measured by the observer with an overhead prime.

Notice that we are not required to specify how the observer has moved along line  $OP$  or the source has moved along the line  $SP$ , that is to say, with uniform velocity or with acceleration. Equations (A4) and (A5) hold generally.

Now, as described on page 142 in French (1966), we can approximate

$$(SP) = u\Delta t' \quad (\text{A6})$$

for  $u$  as 'uniform' velocity. On using equation (A6) in equation (A5), we then obtain

$$\Delta T' = (1 + \beta \cos \theta) \Delta t' \implies \frac{1}{\Delta T'} \equiv \nu_o = \nu_e \frac{\sqrt{1 - \beta^2}}{1 + \beta \cos \theta}, \quad (\text{A7})$$

where we have used  $\beta = u/c$  and that  $\Delta t' = 1/\nu_e \sqrt{1 - \beta^2}$  with  $\nu_e$  being the frequency of the emitted wave in the rest frame of the source. This is the standard formula of equation (A1) or equation (5)–(17) on page 143 of French (1966).

But, eq. (A6) has an error. Distance  $(SP)$  is 'not'  $u\Delta t'$ , but  $(SP) = u\Delta T'$ . The source, if at all it does so, moves only during the period  $\Delta T' = T'_2 - T'_1$ , and not during  $\Delta t = t_2 - t_1$ .



Now, we notice that equation (5) reduces to  $1 \pm \beta$ , the non-special relativistic expressions of the Doppler shift, for  $\theta = 0, \pi$ . On the other hand, the standard formula, equation (A1), reduces to  $\sqrt{\frac{1-\beta}{1+\beta}}$  for  $\theta = 0$  and to  $\sqrt{\frac{1+\beta}{1-\beta}}$  for  $\theta = \pi$ . Equation (5) will not correspond with equation (A1), which is validated by a variety of experiments (Ashby 2003).

Therefore, we have the situation that the standard formula, equation (A1) is well-supported by experiments, but is theoretically inappropriate. Theoretically correct special relativistic formula of equation (A9) gets ruled out by the Ives–Stilwell experiment. However, it is still unclear as to why equation (A1) correspond well with the experimental results.

On the other hand, equation (5) is obtained for the case of constant acceleration, and it disagrees with the standard formula and, hence, with experiments. Further investigations are thus essential for an appropriate resolution of this situation.

We may nevertheless use variable acceleration to express distance (SP) in equation (A5) in terms of appropriate quantities, or as described in section 4, to gain further understanding of the ways of measuring velocity and acceleration of the source from its Doppler shift. This is described in the main body of this paper.

## References

- Ashby, N. 2003, Relativity in the Global Positioning System, *Living Rev. Relativity*, **6**, 1 [online article: <http://www.livingreviews.org/lrr-2003-1>].
- Fabrika, S. 2004, *Astrophysics and Space Physics Reviews*, **12**, 1.
- French, A. P. 1966, *Special Relativity (The MIT Introductory Physics Series)*, W W Norton & Co., New York.
- Ives, H. E., Stilwell, G. R. 1938, *J. Opt. Soc. Am.*, **28**, 215–236.
- Margon, B. 1984, *ARA&A*, **22**, 507.
- Margon, B., Anderson, S. F. 1989, *ApJ*, **347**, 448.
- Marshall, H. L., Canizares, C. R., Hillwig, T., Mioduszewski, A., Rupen, M., Schulz, N. S., Nowak, M., Heinz, S. 2013, Multi-wavelength Observations of the SS433 Jets (to be published in *ApJ*) ([arxiv.org/astro-ph.HE/1307.8427](http://arxiv.org/astro-ph.HE/1307.8427)).
- Mirabel, I. F. 1999, *ARA&A*, **37**, 409.
- Wagh, S. M. 2013a, *Pramana – J. Phys.*, **81(3)**, 439–448 (doi:[10.1007/s12043-013-0584-6](https://doi.org/10.1007/s12043-013-0584-6)).
- Wagh, S. M. 2013b, *J. Modern Physics*, **4(8A)**, 102–104 (doi:[10.4236/jmp.2013.48A008](https://doi.org/10.4236/jmp.2013.48A008)).
- Wagh, S. M. 2013c, Subtlety in relativity, Paper for SPIE Conference on The Nature of Light. What are photons? V – Part of Optics and Photonics Event, paper no. 8832-25, San Diego, California, 25–29 August 2013.
- Wagh, S. M., Sarwe, S. B. 2013, Jets in micro-quasar SS433: Analysis involving acceleration, *J. Astrophys. Aerospace Tech.*, to be published.